International Journal of Combinatorial Optimization Problems and Informatics, 11(3), Sep-Dec 2020, 21-36. ISSN: 2007-1558.

www.editada.org

Applications of Shearography for Non-Destructive Testing and Strain measurement

Fernando Rojas-Vargas [1], Juan Benito Pascual-Francisco [1], Tonatiuh Hernández-Cortés[1]*

[1] Universidad Politécnica de Pachuca, Carretera Pachuca-Cd. Sahagún Km. 20, Ex-Hacienda de Santa Bárbara, 43830, Zempoala, Hidalgo, México.

[*] *juanpascual@upp.edu.mx*

Abstract. Non-Destructive Testing (NDT) technologies have gain importance recently due to the demand of high quality and costs optimization in products. Thus, non-contact optical techniques have been developed, which also have been well accepted in the industry. This work presents a background of developments and applications of shearing speckle pattern interferometry, known as shearography, for NDT analysis. Also, some important experimental results, from authors, for NDT analysis and strain measurement are reported.

Keywords: Shearography, nondestructive testing, speckle interferometry, strain measurement.

Article Info
Received Sep 11, 2019
Accepted Dec 11, 2019

1 Introduction

The high-quality product in the industry, demands improvements in manufacturing processes and quality inspection. In order to assess the quality and functionality of products, many methodologies have been developed. These can be classified into two main groups: Destructive and Non-destructive. Likewise, these methodologies are divided into different techniques. In Non-destructive testing, as the name suggests, the product or mechanical element do not suffer damage and can be put in service after testing. On the other hand, destructive testing implies the partial or total destruction of the material, therefore, the component cannot be put in service anymore and the subsequent negative effect in cost [1]. Due to this, NDT techniques are more attractive for the industry since they avoid the wasting of materials and improve the cost-effectiveness [1-2].

At the same time, the NDT techniques can be divided into two groups: the contact and the non-contact ones. In the first group, there can be found the magnetic particles, penetrating liquids, ultrasound, acoustic emission, etc. For the non-contact exist the whole field optical techniques, such as interferometric-based techniques and Digital Image Correlation (DIC) [3]. These allow the analysis of the entire or a part of the surface of the object under study [4, 5]. Among the interferometry-based techniques, it can be found the electronic speckle pattern shearing interferometry, also known as shearography. This technique is based on light interference and the speckle phenomenon of laser light sources [6-7]. It has been demonstrated that shearography is a powerful tool for NDT inspection and its applications are rapidly increasing [8-10], for example: Application for quality inspection in the tire industry [11], in the aerospace for the detection of damage in turbine blades and in the fuselage of planes [12-13], in detection of cracks in pipes [14], and also is used for strain measurement for the characterization of mechanical properties of materials since its provides the strain field [15-20]. In further sections, the basic principles of shearography are derived and some cases of study of the application are presented. Moreover, the results of some experiments, carried out by the authors, are added in order to provide de adaptability and the effectiveness of this technique.

2 Principles of Shearography

Shearography, as well as other interferometric techniques, such as electronic speckle pattern interferometry, is based on the principles of the light interference and the speckle phenomenon. When an object surface is illuminated with an expanded laser beam, it can be observed a grainy appearance over the illuminated area, which consist of bright dark spots. This speckle pattern is due to the random interference of the scattered light beam by the surface [21]. So, in an initial state, there will be a reference speckle pattern. If the object is loaded, its surface will be deformed, which also induces a change in the speckle pattern. With a convenient experimental set-up, the information of the displacement or strain suffered by the object can be obtained by subtracting

the image of the deformed state from the reference state [22]. In Figure 1, a characteristic speckle pattern scattered by an object surface is presented.

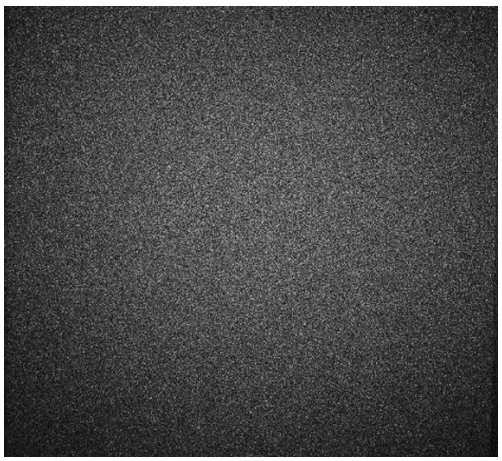

Figure 1. Speckle pattern obtained with an expanded laser beam.

A typical shearography set-up is based on the Michelson interferometer [23]. In its basic form, it consists of a laser light source, an image acquisition device (commonly a CCD camera), a beam splitter and two mirrors. One of the mirrors is slightly tilted in order to produce an effect of two sheared image of the same image on the sensor of the camera. In Figure 2, the basic shearography set-up, as well as the effect of the shearing mirror on the camera is illustrated.

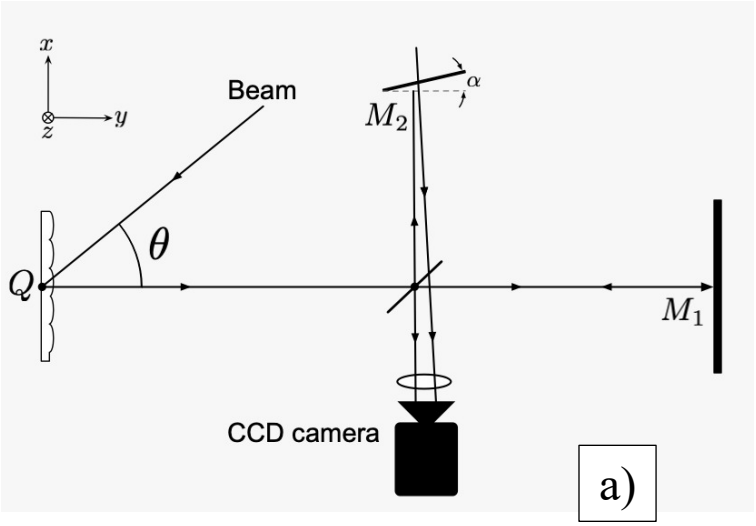

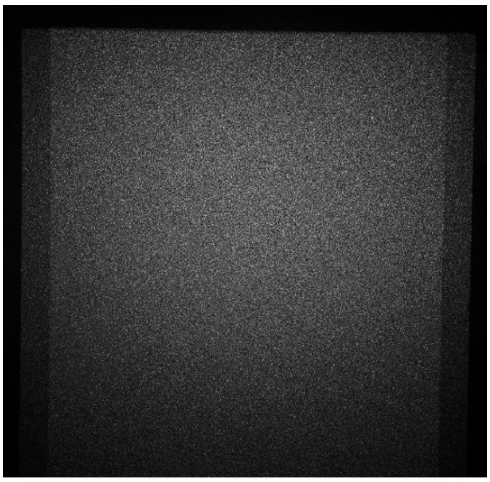

Figure 2. a) Shearography set-up based on a modified Michelson interferometer; b) the result of tilting one of the mirrors, producing the overlapping of two images of the same object, producing a shearing effect.

When the image of the deformed object is subtracted from the reference state, a fringe pattern known as shearogram is obtained. A typical shearogram obtained in this process is shown in Figure 3. So, if the object suffers a deformation, this is revealed as the appearing of this fringe pattern.

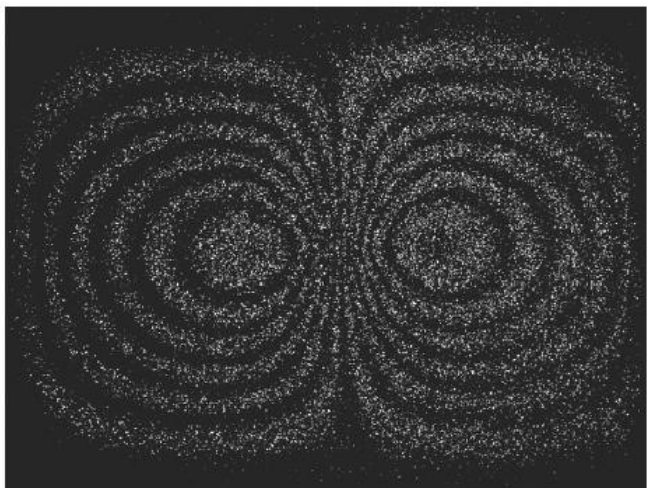

Figure 3. A shearogram obtained with the subtraction of two shearing speckle patterns.

3 Relationship between the deformation of the surface and a phase change in the light intensity

When deformation is induced on the object, the speckle pattern will suffer changes, which also introduces a phase difference in the light intensity registered by the CCD camera. This phase difference related to the deformation is expressed by the fundamental equation of shearography as follows [11].

$$\Delta\varphi = (k_x \frac{\partial u}{\partial y} + k_y \frac{\partial v}{\partial y} + k_z \frac{\partial w}{\partial y})\delta y \tag{1}$$

Where k_x, k_y and k_z are the sensitivity vector in the corresponding x, y and z direction; $\frac{\partial u}{\partial y}$, $\frac{\partial v}{\partial y}$ and $\frac{\partial w}{\partial y}$ are the derivative of displacements, and δy is the shearing distance introduces bye tilting one of the mirrors in the y direction. Though it is not marked explicitly in equation (1), the phase is in function on the location of the point on the object surface P(x,y). Also, equation (1) shows that there are three variables that contribute to the determination of the phase. The deformation of the object is represented as derivatives of displacement in the direction of the shearing distance δy. The direction of the illumination and observation and the wavelength of the laser determine the sensitivity vector $\boldsymbol{k}$. The third contribution is the shearing distance δy introduced by the tilted mirror in the modified Michelson interferometer. With this last variable, shearography allows the adjustment of the sensibility to the detection of deformations. With a small shearing distance, the sensibility is reduced, while with high value the sensitivity increases. However, with a large shearing distance the approximation to the derivative is highly affected, which compromises the accuracy in quantitative strain measurements, since strain is the derivative of displacement.
If the illumination remain in the plane $x - z$, as shown in Figure 4, the sensitivity vector can be defined as

$$|\boldsymbol{k}_s| = \frac{4\pi}{\lambda}\cos\frac{\theta_{xz}}{2} \tag{2}$$

Where λ is the wavelength and θ_{xz} is the illumination angle in the $x - z$ plane.

From Figure 4, the respective sensitivity vector in the three directions is as follows.

$$k_x = k_s e_x = |\boldsymbol{k}_s| \sin\frac{\theta_{xz}}{2} = \frac{4\pi}{\lambda}\cos\frac{\theta_{xz}}{2}\left(\sin\frac{\theta_{xz}}{2}\right) = \frac{2\pi}{\lambda}\sin\theta_{xz} \tag{3}$$

$$k_y = k_s e_y = 0 \tag{4}$$

$$k_z = k_s e_z = |\boldsymbol{k}_s| \cos\theta_{xz} = \frac{4\pi}{\lambda}\cos\frac{\theta_{xz}}{2}\left(\cos\frac{\theta_{xz}}{2}\right) = \frac{2\pi}{\lambda}(1+\cos\theta_{xz}) \tag{5}$$

So, the fundamental equation of shearography will be as follows.

$$\Delta\varphi_y = \frac{2\pi}{\lambda}\left[\sin\theta_{xz}\frac{\partial u}{\partial y} + (1+\cos\theta_{xz})\frac{\partial w}{\partial y}\right]\delta y \tag{6}$$

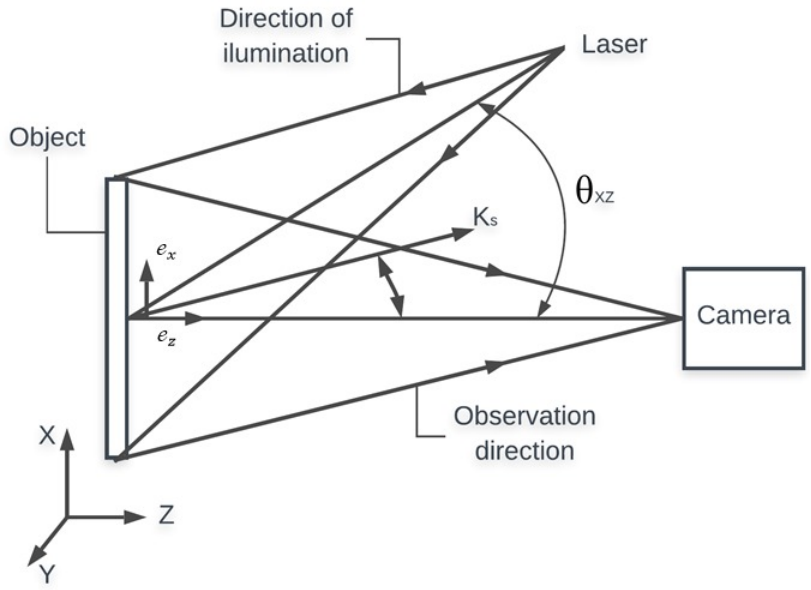

Figure 4. Sensitivity vector of a point over the object surface.

If the mirror is tilted in the x direction, equation 6 becomes:

$$\Delta\varphi_x = \frac{2\pi}{\lambda}\left[\sin\theta_{xz}\frac{\partial u}{\partial x} + (1+\cos\theta_{xz})\frac{\partial w}{\partial x}\right]\delta x \tag{7}$$

Equation (6) or (7) show that a shearogram contain information of both in-plane and out-of-plane components of the strain tensor, which has the form:

$$\begin{vmatrix} \varepsilon_{xx} & \varepsilon_{xy} & \varepsilon_{xz} \\ \varepsilon_{yx} & \varepsilon_{yy} & \varepsilon_{yz} \\ \varepsilon_{zx} & \varepsilon_{zy} & \varepsilon_{zz} \end{vmatrix} = \begin{vmatrix} \frac{\partial u}{\partial x} & \frac{1}{2}\left(\frac{\partial u}{\partial y}+\frac{\partial v}{\partial x}\right) & \frac{1}{2}\left(\frac{\partial u}{\partial z}+\frac{\partial w}{\partial x}\right) \\ \frac{1}{2}\left(\frac{\partial v}{\partial x}+\frac{\partial u}{\partial y}\right) & \frac{\partial v}{\partial y} & \frac{1}{2}\left(\frac{\partial v}{\partial z}+\frac{\partial w}{\partial y}\right) \\ \frac{1}{2}\left(\frac{\partial w}{\partial x}+\frac{\partial u}{\partial z}\right) & \frac{1}{2}\left(\frac{\partial w}{\partial y}+\frac{\partial v}{\partial z}\right) & \frac{\partial w}{\partial z} \end{vmatrix} \tag{8}$$

Where ε_{xx}, ε_{yy} and ε_{zz} are the normal strain components in the x, y and z, respectively and the rest represent the shearing strains.

So, it can be observed that if the illumination plane remains in the $x-z$ plane, and the shearing is in the x direction, the normal strain ε_{xx} can be obtained as well as component of the shearing strain $\frac{\partial w}{\partial x}$, which also represents an out-of-plane displacement derivative. On the other hand, if the illumination is in the $y-z$ plane, it is possible to obtain the normal strain component ε_{yy} by tilting the mirror in the y direction. This is the reason that shearography can be used for whole field strain measurement.
As mentioned above, the fundamental equation contains both in-plane and out-of-plane strain components. When the illumination is adjusted normal to the object surface, the angle of illumination tends to cero. In this particular case, equation (6) and (7) become:

$$\Delta\varphi_y = \frac{4\pi\delta y}{\lambda}\frac{\partial w}{\partial y} \tag{9}$$

$$\Delta\varphi_x = \frac{4\pi\delta x}{\lambda}\frac{\partial w}{\partial x} \tag{10}$$

It is known that in interferometry, every fringe pattern has a period of $2\pi n$, where n is the fringe number [4]. This means that every time the phase is 2π there will exist a fringe in the shearogram. So with equation (9) and (10), the out-of-plane displacement derivative can be computed by counting the number of fringes on the shearogram. Equations (9) and (10) become:

$$\frac{\partial w}{\partial y} = \frac{\lambda n}{2\delta y} \tag{11}$$

$$\frac{\partial w}{\partial x} = \frac{\lambda n}{2n\delta x} \tag{12}$$

These last equations are the base upon which shearography is established for NDT analysis. This is because a flaw, an inner crack or an imperfection of the material will cause a higher gradient of deformation than the in rest of the object when it is loaded. This gradient of deformation is associated with the fringe patterns, which are obtained by subtracting images of deformed states from the reference. Fortunately, this process can be performed in real-time.

4 Shearography for NDT analysis

In the last section, the fundamental equations of shearography were derived. With either equation (11) or equation (12), NDT analysis can be performed. In Figure 5, a typical experimental set-up of shearography for NDT analysis is presented. The expanded laser beam will illuminate the object surface at an angle approximated to cero. This is important to achieve so that equation (11) can be applied, as pointed out above.

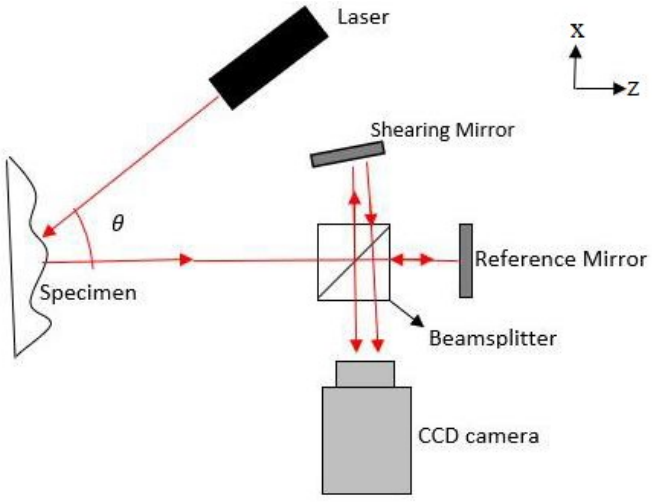

Figure 5. Sensitivity vector of a point over the object surface.

Flaw revelation by shearography is based on the comparison of two states of deformation in the test object. Development of nondestructive testing procedures employing shearography essentially becomes the development of a practical means of stressing

which can reveal flaws [24-26]. Ideally, it is desirable to impose stresses similar to the stress-state found in service. If components under testing are loaded in a stress mode similar to the actual one experienced in service, shearography can be used to reveal critical flaws only (i.e. flaws that create strain concentrations and thus reduce the strength of the component) [24]. Cosmetic flaws can be ignored, and false rejects can be avoided. Examples of cosmetic flaws include those located in low-stress regions which will not jeopardize the strength of the structures. Exact duplication of the actual stress-increment for shearographic testing, however, is generally difficult. Therefore, various practical means of stressing the object must be developed. In developing these methods, an important precaution to be taken is restricting rigid-body motion of the object during stressing, as excessive rigid-body motion would cause speckles de-correlation, resulting in degradation of fringe quality [27-28].

One of the most important applications of digital shearography for NDT since its early beginnings was the study of delamination in composite materials. Composites constructed as honeycomb panel usually suffer delamination when subjected to loads and corrosive medium. For this, Huang, et al. [24] have performed some experiments. Figure 6 depicts several delaminations in a honeycomb panel. The skin of the panel is graphite epoxy. The means of stressing is a partial vacuum.

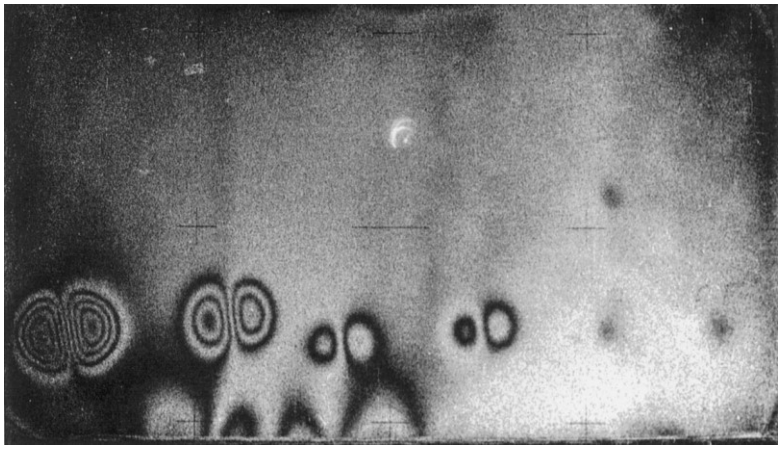

Figure 6. Revealing several delaminations in a honeycomb panel [24].

Another application of shearography reported is the detection of inner crack in pressure vessels [15]. Figure 7 shows fringe correlations revealing a localized crack in the material. The means of stressing is internal pressurization.

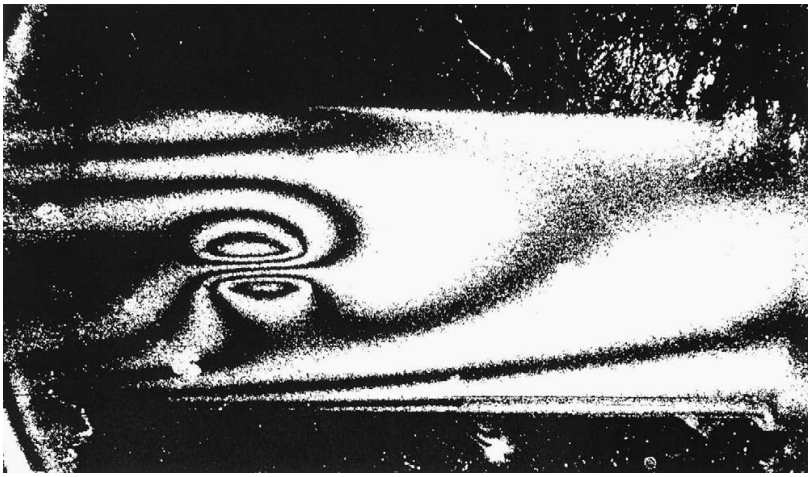

Figure 7. Detection of internal cracks in a pressure vessel [15].

Another experiment reported is the detection of a crack by thermal stressing [24, 29, 30]. A square aluminium plate with a subsurface vertical crack as shown in Figure 8(a) is first used to demonstrate the capability of the proposed method. The plate is fully clamped on four edges and a heat flux of 9.6 kWs is then triggered in front of the plate. Speckle images before and after the heat pulse are captured and phase information are obtained using the proposed clustering method. Figure 8(b) shows a

shearographic fringe map of the plate. The crack-induced deformation anomaly is clearly seen and a vertical crack is easily identified in the fringe map.

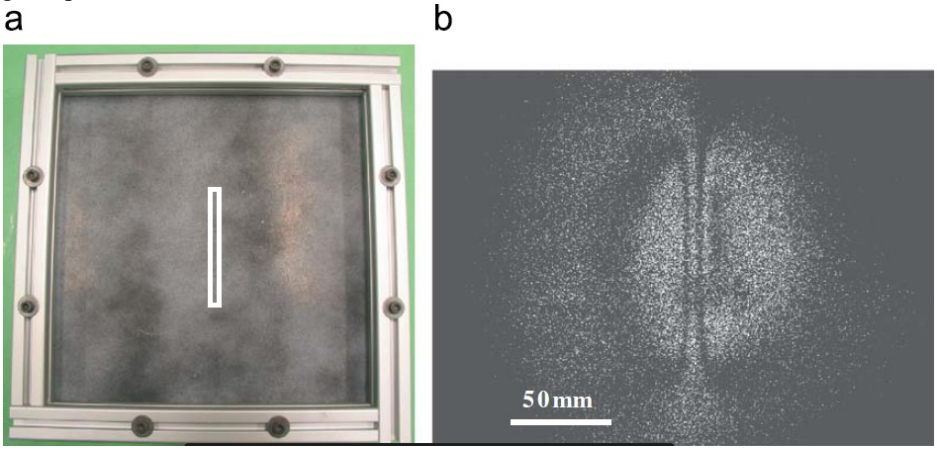

Figure 8. (a) An aluminium plate with a vertical crack at the back center indicated in with the white rectangle. (b) Fringe pattern obtained with shearography depicting a vertical crack [24].

Also, [24] reported the result of evaluating internal cracks in pressure pipes and in open-ended pipes. Authors proposed that for pressure pipes, the best stressing method is by either vacuum o by applying pressure. Figure 9 shows the result obtained by applying the pressure method in a PVC pipe with an internal crack. Also, the same authors reported the results of applying the thermal method to reveal horizontal and vertical inner crack in an open-ended PVC pipe. This result is illustrated in Figure 10.

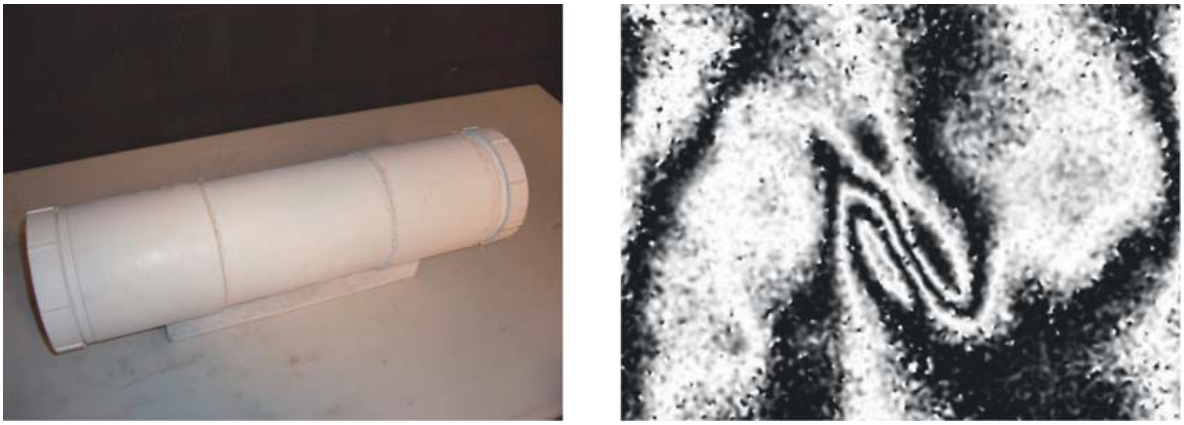

Figure 9. Revealing internal crack in a PVC pipe with the pressure method [24].

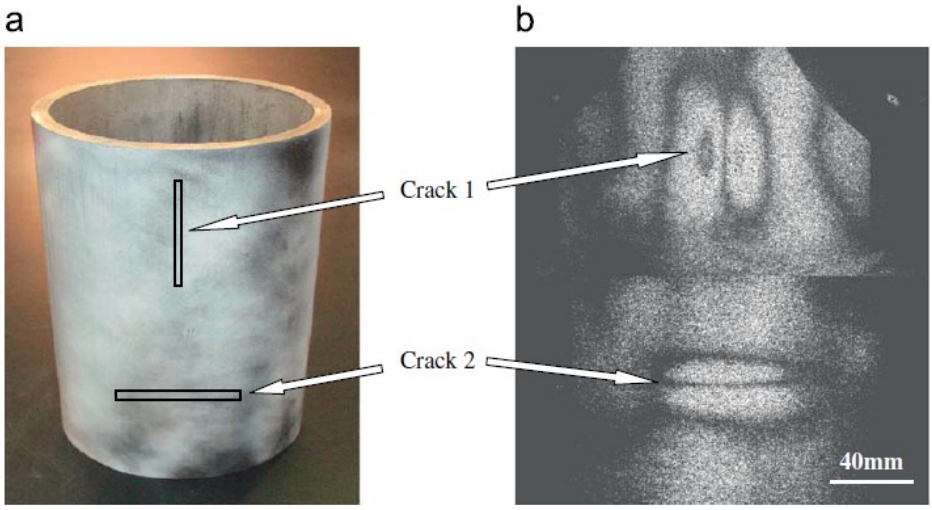

Figure 10. Revealing vertical and horizontal inner cracks via thermal stressing [24].

A very important advance of shearography for NDT is the work reported by Francis et al. [12]. They employed shearography to evaluate an aeroplane panel that experienced damage due to a hailstorm. The measurements were made with a single-component, out-of-plane displacement gradient sensitive shearography system. A region of the surface of the panel with an area of approximately 50 cm2 was loaded thermally using an infrared source. Figure 11 illustrates the results obtained. It can be observed that the damages are revealed as fringe patterns in the evaluated area.

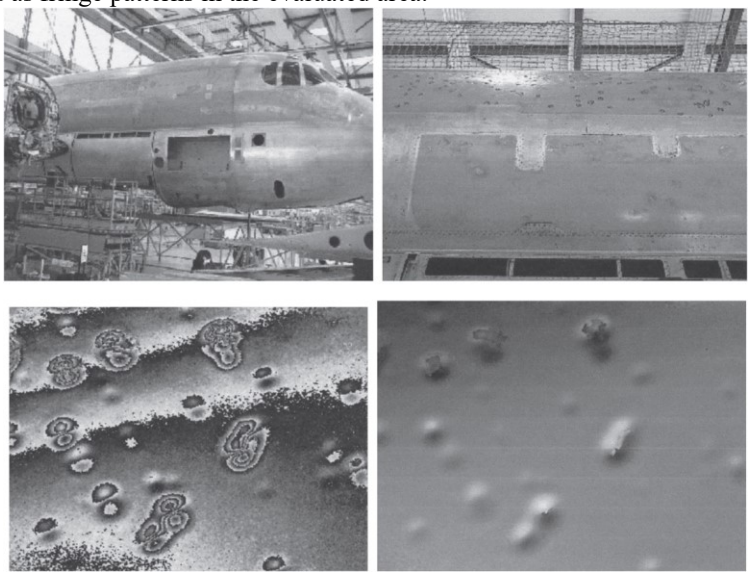

Figure 11. Evaluating damage in an aeroplane panel caused by hailstorm [12].

5 Shearography for quantitative analysis

Another approach of shearography is quantitative evaluation. This means that the phase change induced by a deformations is computed [31]. This also implies that the strain measurement can be performed. For this approach, the main issue is to find out a methodology to quantitative measure the phase maps. This is very important because by obtaining the phase map, the full-field strain distribution can be obtained [32]. The most popular method for phase measurement is well known as phase-shifting [33]. This consists of capturing a series of images of the object and introducing a phase change in the light intensity for each of them. Commonly, this phase change is introduced by translating one of the mirrors of the interferometer. This movement can be achieved by applying a voltage to a Piezo-crystal (PZT) attached to the mirror. A phase-shifting shearography experimental set-up is the same as the conventional, with the only difference that the un-tilted mirror is attached to a PZT with a Piezo controller [34]. The

image acquisition must be synchronized with the application of the voltage to the PZT [35]. Figure 12 shows a diagram of the phase-shifting shearography set-up. In the modified Michelson interferometer the two sheared images interfere with each other producing a resultant speckled image with intensity distribution given by:

$$I(x,y) = a(x,y) + b(x,y)\ \cos\varphi \tag{13}$$

where a is the background intensity, which depicts the average spatial intensity; b is a modulation term and φ is a random phase angle. When the object is deformed, an optical path change occurs due to the surface displacement of the object. This optical path change induces a relative phase change between the two interfering points. Thus, the intensity distribution of the speckle pattern is slightly altered and is mathematically represented by

$$I' = a(x,y) + b(x,y)\ \cos\varphi' \tag{14}$$
$$\varphi' = \varphi + \phi$$

where I' is the intensity distribution after deformation, and ϕ is the phase change due to the deformation. As expressed in equations (13) and (14), the terms a, b, and φ depend on their location (x,y) on the image.

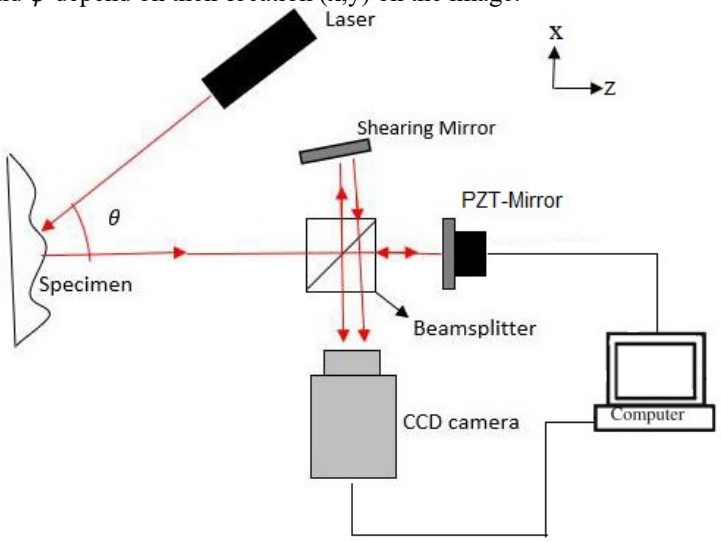

Figure 12. Phase-shifting shearography set-up for quantitative analysis

As mentioned above, for quantitative analysis usually the phase-shifting method is employed to the determination of the phase distribution. The three, four, and five-step phase shift algorithms are the common temporal phase shift algorithms. However, the most popular is the four-step algorithm [13]. Phase shifting of $\frac{\pi}{2}$ is introduced by translating one of the mirrors in the interferometer by means of a piezoelectric crystal (PZT). Thus, for dereference state, simplifying equation (13), the intensity distributions of the four frames are expressed as [11]:

$$I_1 = a + b\cos\varphi \tag{15}$$
$$I_2 = a + b\cos\left(\varphi + \frac{\pi}{2}\right) \tag{16}$$
$$I_3 = a + b\cos(\varphi + \pi) \tag{17}$$
$$I_4 = a + b\cos\left(\varphi + \frac{3\pi}{2}\right) \tag{18}$$

Solving (15)-(18) one can obtain the equation for the phase distribution

$$\varphi = \tan^{-1}\frac{I_4 - I_2}{I_1 - I_3} \tag{19}$$

The same process is applied to the deformed state. The relative phase difference $(\varphi - \varphi')$ between the reference and the deformed state gives the information on the derivatives of displacements. Once this phase map has been obtained, the derivatives of displacement, given by equations (6), (7), (9) and (10), can be finally computed.

5.1 In-plane strain measurement

One of the most attractive applications of shearography in experimental mechanics is the full-field strain measurement [36, 37]. For this purpose, the in-plane strain component has to be isolated from equation (7), which is $\varepsilon_{xx} = \frac{\partial u}{\partial x}$. For this a special experimental, a dual illumination system has to be implemented set-up as illustrated in Figure 13 [38, 39]. Particularly, with this set-up the strains in the x direction can be obtained.

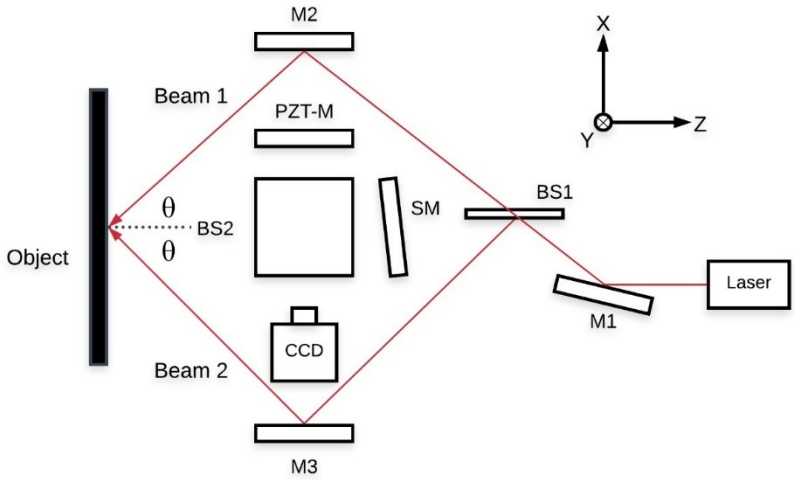

Figure 13. Experimental shearography set-up for in-plane strain measurement. M1, M2 and M3: mirrors; PZT-M: piezo crystal mirror; SM: shearing mirror; BS1, BS2: beam splitters; θ: incident angle.

In order to eliminate the out-of-plane component from equation (7), two laser beams are used. The object is illuminated sequentially and the phase-shifting technique is performed for each beam [40]. Consequently, two relative phase difference are obtained. Rewritten equation (7) for the two incident beams, these are:

$$\Delta_1 = \frac{2\pi}{\lambda}\left[\sin\theta\frac{\partial u}{\partial x} + (1+\cos\theta)\frac{\partial w}{\partial y}\right]\delta_x \tag{20}$$

$$\Delta_2 = \frac{2\pi}{\lambda}\left[\sin\theta\frac{\partial u}{\partial x} + (1+\cos\theta)\frac{\partial w}{\partial y}\right]\delta_x \tag{21}$$

Subtracting (21) from (20), finally, the in-plane strain component can be isolated [15].

$$\Delta_1 - \Delta_2 = \frac{4\pi}{\lambda}\left(\sin\theta\frac{\partial u}{\partial x}\right)\delta_x \tag{22}$$

Thus, the component of strain ε_{xx} is calculated by the next equation:

$$\varepsilon_{xx} = \frac{\lambda}{4\pi}\frac{(\Delta_1 - \Delta_2)}{\delta_x \sin\theta} \tag{23}$$

The strain measurement using shearography is being well accepted in experimental mechanics because of its adaptability and the advantage of providing full-field information. So, in literature, many applications of shearography for strain measurement have been reported [41-45].

6 Cases of Study

In order to demonstrate the potential of shearography for NDT analysis and strain measurement, authors have performed two experiments. The first is regarding the detection of an internal crack in a PVC pipe by stressing with pressure. The second experiments is the measurement of the strain field in an elastomer subjected to tension stress.

6.1 Detection of internal crack in real-time

In this experiment, an artificial crack generated in the inner surface of the PVC pipe. The aim is to reveal this crack with the experimental set-up shown in Figure 14. The mean of stressing was pressurization. In order to expand the laser beam over the pipe's surface, a diffusor glass was employed.

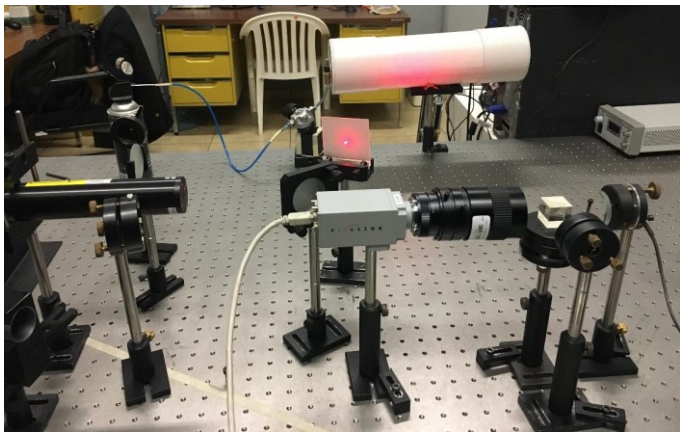

Figure 14. The fringe pattern generated in the region where an internal crack was produced.

The image acquisition and the image processing were performed in real-time with a program written in LabVIEW. In the reference state, no load is applied to the material. Then, the pressure was applied gradually and the image started at the same time. Image acquisition was set at a frame rate of 1fps. The software performed the image subtraction instantly when images are acquired. In resulting correlated fringes are displayed on the screen, where the evolution of the fringes can be observed when pressure is gradually increased. In Figure 15, a fringe pattern produced in the region of the crack can be observed. This simple experiment demonstrates the effectiveness of shearography for inner crack detection. This methodology can be used for NDT for pressure vessels in the industry in order to evaluate their integrity. Another application of this method, which at this time is a future challenge, is the real-time evaluation in pipelines in the oil industry [46]. For this, it is essential to develop portable devices that can be adapted to the real field [47]. Recently, some portable shearography equipment are being developed by companies or institutions [48-50]. So, in a not far future, more and novel applications of shearography in the industry are expected to be published.

Figure 15. The fringe pattern generated in the region where an internal crack was produced.

6.2 Strain measurement in elastomers

Many authors have reported results of strain measurement with shearography. However, they are focused on measuring strain in metals, composites, ceramics, and concrete. So, authors have explored the effectiveness of this optical technique to measure the strain field in elastomers. In this new application, a viscoelastic property of elastomers, known as creep, was evaluated. The creep is a time-dependent viscoelastic mechanical property of materials when subjected to a constant load for prolonged periods of time. Particularly, elastomers can experience large deformations when they are working with a load for thousands of hours of service. Even if the load do not increase, these kind of materials can suffer a fracture. So studying this phenomenon is very important for the prediction of the service life of this polymer, which are commonly used as sealing elements in machinery. Thus, in order to demonstrate the effectiveness of shearography in this kind of application, short-term creep tests of 3 hours were performed. Silicone rubber is the most common elastomer used as a seal, so this was chosen in this case.

Figure 16 shows the shearography experimental set-up implemented in this study. First, the test specimen was clamped to a structure. In front of the specimen, the shearography and the illumination systems were installed. The camera lens was focused on the test object throughout the Michelson interferometer so that the whole gauge length was fully visualized. To produce the shearing effect one of the mirrors (M4) of the Michelson interferometer was slightly tilted. A PZT crystal was incorporated into the other mirror (M5) in order to perform the phase shifting. As to the illumination system, a 630 nm Helium-Neon laser was utilized. The laser beam passes through microscopy objective (MO) in order to get an expanded beam. Then it is reflected on mirror M1 to the beam splitter BS1, in which the beam is divided into two parts. Beam 1 and beam 2 are reflected by mirrors M2 and M3, respectively, to coincide on the object surface at an angle of 18.5 degrees with respect to the optical axis. Image acquisition and phase-shifting were made by using LabVIEW and the image processing was performed in MATLAB.

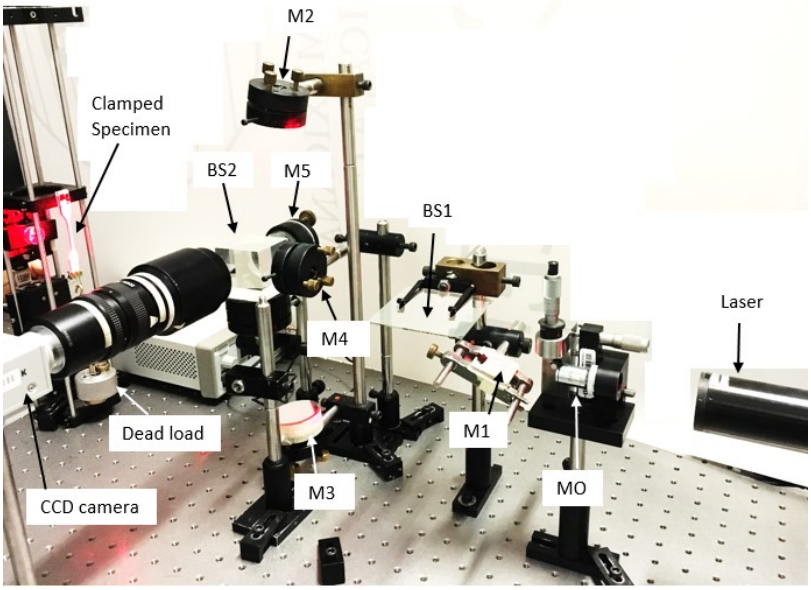

Figure 16. Experimental shearography setup implemented.

Then, the dead load was gently applied to the free end of the test. Besides the gently application of the load, it was necessary to start the measurements after 30 seconds, while the specimen was stabilized. Due to that, the deformation occurs quickly during the first minutes, the strains were measured every minute during 30 minutes. After 30 minutes, the strain rate decreases considerably, so measurements were performed each 3 minutes until the 3 hours were completed.

In order to get only the strain information on the gauge length, a rectangle mask was created over the image of the gauge specimen as shown in Figure 17. Then, the average strain value at each sampling is computed and tabulated. The result of the creep strain is presented in Figure 18, in which the characteristic creep curve can be observed [51, 52].

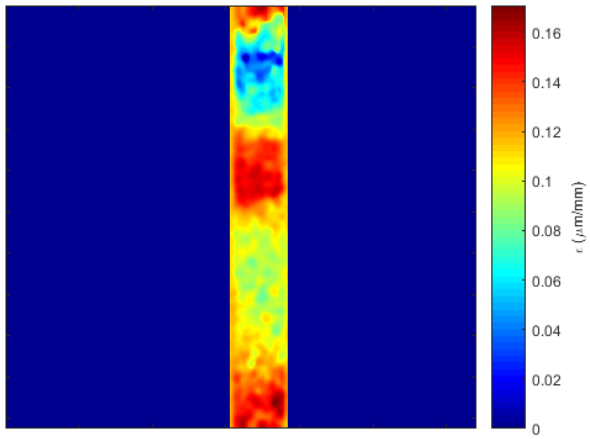

Figure 17. Strain distribution obtained with shearography.

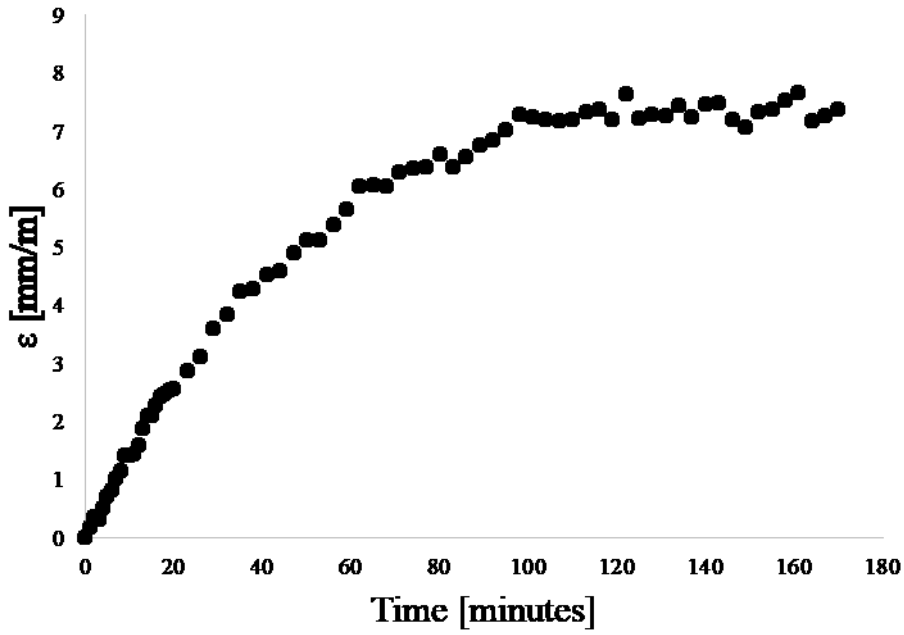

Figure 18. Creep strain curve obtained with shearography.

From the results obtained can be clearly seen that this optical full-field technique is also effective for strain measurement not only in metals or composites but in elastomers. So, shearography can be applied for the assessment and characterization of mechanical properties of materials.

7 Conclusions

In this paper, the basic theory of shearography was presented. The fundamental equations of this technique for NDT analysis and strain measurement were derived. Then, some applications for NDT analysis reported in the literature were presented. It was shown that shearography is a powerful tool for the detection of cracks or flaws in any kind of materials. Finally, two cases of study of the applications of shearography carried out by the authors were described: one for the qualitative NDT approach and one for the quantitative approach. With the results, obtained authors have demonstrated that shearography is a very effective technique for either NDT analysis or strain measurement. It was also pointed out that one of the challenges of this optical technique is to develop portable devices for in-situ analysis. So, in a few years, new and novel applications of shearography are expected to be reported.

Acknowledgements

The authors thank “Laboratorio de pruebas ópticas y mecánicas” from Centro de Investigaciones en Óptica, León Guanajuato, México, for allowing using the optical components in the experiments.

References

[1] S.Gholizadeh (2016). A review of non-destructive testing methods of composite materials. Structural Integrity Procedia 1, 50-57.

[2] Gholizadeh S. (2016). A review of non-destructive testing methods of composite materials. Procedia Structural Integrity 1, 50-57.

[3] Farfán Cabrera L I, Pascual Francisco J B Barragán Pérez O, Gallardo Hernández E A, Susarrey Huerta O (2017). Determination of creep compliance, recovery and Poisson's ratio of elastomers by means of digital image correlation (DIC). Polym Testing. 59: 245-252.

[4] Sirohi Rajpal (2009). Optical methods of measurement wholefield techniques. Second edition, CRC Press.

[5] Rabal J. H., Braga Jr. and Roberto A. (2009) Dynamic Laser Speckle and Application. CRC Press

[6] Leendertz, J. A. (1970) Interferometric displacement measurement on scattering surfaces utilizing speckle effect. J. Phys. E: Sci. Instrum. 3, 214-218.

[7] Hung, Y.Y. (1974). A speckle interferometer: a tool for measuring derivatives of surface displacement. Opt. Commun. 11(2), 132-135.

[8] Liu H. et al. (2018). Directed acoustic shearography for crack detection around fastener holes in aluminum plates. NDT &E International 110, 124-131.

[9] Yan P. et al. (2019). Shearography for non-destructive testing of specular reflecting objects using scattered light illumination. Optics & Laser Technology 112, 452-457.

[10] Liu Z., Gao J., Xie H., Wallace P. (2011). NDT capability of digital shearography for different materials. Optics and lasers in Engineering 49, 1462-1469.

[11] Steinchen W., Yang L. (2003). Digital shearography, SPIE Press, Bellingham Washington USA.

[12] D. Francis, R. P. Tatam, and R. M. Groves (2010) Shearography technology and applications: a review. Meas. Sci. Technol. 21, 102001

[13] Yusnisyam M. et al. (2019). Shearography Technique on Inspection of Advanced Aircraft Composite Material. IOP Conference Series: Materials Science and Engineering (554) 012009.

[14] Liu B. et al. (2017). Inspection of the interior surface of cylindrical vessels using optic fiber shearography. Measurement Science and Technology 28 095202.

[15] Hung Y., Ho H. (2005). Shearography: An optical measurement technique and applications. Materials Science and Engineering 49, 61-87.

[16] Martínez A, Rayas J A, Cordero R, and Labbe F (2011). Comparative measurement of in plane strain by shearography and Electronic speckle pattern interferometry. Rev Mex Fís. 57: 518-523.

[17] Hung, Y.Y. (1982). Shearography: a new optical method for strain measurement and nondestructive testing. Opt. Eng. 21(3), 391-395

[18] Pascual Francisco J. B. et.al. (2017). The effectiveness of Shearography and Digital Image Correlation for the study of creep in elastomers Mater. Res. Express 4 115301.

[19] Omar Barragán-Pérez, Juan Benito Pascual-Francisco, Orlando Susarrey-Huerta. (2019). *Shearography as a tool to measure creep strain in sealing elastomers*. Rev. Mex. Fis 65 (5) 583-589.

[20] Kim H. J., Gweon D. G. y Kim H. C. (2012) Development of the integrated measurement system of strain distribution and defect using ESPI and Shearography. International Journal of precision engineering and manufacturing, 13 (11) 1931-1939.

[21] Oliver B.M. (1962) Sparkling spots and random diffraction. Proceedings of the IEEE, 51(1) 220-221.

[22] Giuseppe S. S., Martocchia A y Papalillo D. (2012). Simple educational tool for digital speckle Shearography. Eur. J. Phys. 33, 733-750

[23] J. A. Leendertz and J. N. Butters (1973). An image-shearing speckle-pattern interferometer for measuring bending moments. J. Phys. E: Sci. Instrum. (6) 1107

[24] Y. H. Huang, S .P .Ng, L. Liu, C. L. Li, Y. S. Chen and Y. Y. Hung. (2009). NDT&E using shearography with impulsive thermal stressing and clustering phase extraction. Optics and Lasers in Engineering 47 774–781

[25] Hung Y., Nelson N., Rolly N., Shepard S. (2007). Review and comparison of shearography and pulsed thermography for adhesive bond evaluation. Optical Engineering 46(5), 051007

[26] Y. Y. Hung. (1989). Shearography: A Novel and Practical Approach for Nondestructive Inspection. Journal of Nondestructive Evaluation, VoL 8, No. 2.

[27] Zhu L., Wang Y., Xu N. (2013). Real-time monitoring of phase maps of digital shearography. Optical Engineering 52 (10), 101902.

[28] Y. Y. Hung, W. D. Luo, L. Lin, H. M. Shang (2000). Evaluating the soundness of bonding using shearography. Composite Structures 50 353-362

[29] J. L. Champion, J. B. Spicer, R. Osiander, J. W. M. Spicer, Shearographic Monitoring of Time-Dependent Thermoelastic Deformations, Research in Nondestructive Evaluation 13 (4) (2001) 173-187

[30] Eduardo C. Krutul, Roger M. Groves. (2011). Opto-mechanical modelling and experimental approach to the measurement of aerospace materials using shearography and thermal loading. Proc. of SPIE Vol. 8083 80831C-1

[31] Manuel Servin, J. Antonio Quiroga, and J. Moises Padilla (2014). Fringe Pattern Analysis for Optical Metrology Theory, Algorithms, and Applications. Wiley-VCH, Germany.

[32] Katherine Creath. (1991). Phase-measurement interferometry Techniques for nondestructive testing. Proc. SPIE 1554, Second International Conference on Photomechanics and Speckle Metrology.

[33] Creath, K. (1985). Phase-shifting speckle interferometry. Applied Optics, 24(8) 3053-3058.

[34] S. Waldner. (2000). Quantitative Strain Measurement with Image-Shearing Speckle Pattern Interferometry (Shearography), Diss. Techn. Wiss. ETH Zurich, No 13469.

[35] Zhao Q., et al. (2018). Digital Shearography for NDT: Phase Measurement Technique and Recent Developments. Applied Science 8, 2662.

[36] Francis D., Waldner S. and Tatam R. P., "Surface strain measurement using multi-component shearography with coherent fibre-optic imaging bundles". Meas. Sci. Technol. 18, 3583–91 (2007).

[37] Hung M. Y. Y., Long K. W., Wang J. Q. "Measurement of residual stress by phase shift shearography," Opt Lasers Eng. 27(1),61-73 (1997).

[38] Xie X., et al. (2015). Measurement of in-plane strain with dual beam spatial phase-shift digital shearography. Measurement Science and Technology 26, 115202.

[39] Martínez A., Rayas J. A., Cordero R., and Labbe F., "Comparative measurement of in plane strain by shearography and Electronic speckle pattern interferometry," Rev Mex Fís. 57, 518–523 (2011).

[40] Tyer J., Petzing J. (1997). In-plane Electronic Speckle Pattern Shearing Interferometry. Optics and Lasers in Engineering 26, 395-406.

[41] Hung M., Long K., Wang J. (1997). Measurement of Residual Stress by Phase Shift Shearography. Optics and Lasers in Engineering 27, 61-73.

[42] Fernando Labbe, Raúl R Cordero, Amalia Martínez. (2005). Measuring displacement derivatives by electronic speckle pattern shearing interferometry (ESPSI)

[43] Stephen W. et al. (2000). Surface Strain Characterisation Using Time-Division-Multiplexed 3D Shearography. Proceedigns of SPIE 4101, 389-398.

[44] S. Waldner, S. Brem. (1999). Compact Shearography System for the Measurement of 3D Deformation. Interferometry. SPIE Proc.3745, 141-148

[45] Juan Benito Pascual-Francisco; Orlando Susarrey-Huerta; Alexandre Michtchenko; Omar Barragán-Pérez. (2018). Measurement of creep strain in polymers by means of electronic speckle pattern shearing interferometry. Proceedings Volume 10667, Dimensional Optical Metrology and Inspection for Practical Applications VII; 106670H

[46] Feng X., He X. Y., Tian Ch. P., Zhou H. H. (2014). Research on Inner Defect Detection of Pressure Vessels with Digital Shearography. Proc. of SPIE Vol. 9302 93023J-1

[47] Roger M. Groves, Giancarlo Pedrini, and Wolfgang Osten. (2008). Real-time extended dynamic range imaging in shearography. APPLIED OPTICS Vol. 47, No. 30.

[48] Dirk Findeis, Oliver Hobson, and Jasson Gryzagoridis. (2014). Low Cost Digital Shearography Prototype. Conference Proceedings of the Society for Experimental Mechanics Series, Advancement of Optical Methods in Experimental Mechanics, Volume 3,

[49] Andhee A (2005) A novel compact shearographic NDT system, Master's thesis, University of Cape Town.

[50] Findeis D, Gryzagoridis J, Xaba E, Reid-Rowland D (2000) Aircraft tire inspection using portable shearography and electronic speckle pattern interferometry. Non-Destructive Testing Laboratory, University of Cape Town.

[51] Findley. (2014). Seals and sealing handbook. 6th Edition, Elsevier Science Publishers Limited, England.

[52] Findley W. N., Lai J. S., Onaran K. (1989). Creep and relaxation of nonlinear viscoelastic materials, Dover publications, USA New York.